

# Revisiting Emulsion Polymerization to Produce Stable, Translucent, Nanolatex of Partially Water-Soluble Monomers, Ethylacrylate–Methylmethacrylate

Sumit Bhawal,<sup>1</sup> Deepa Dhoble,<sup>2</sup> Surekha Devi<sup>1</sup>

<sup>1</sup>Department of Chemistry, Faculty of Science, M.S. University, Baroda 390002, India

<sup>2</sup>Polymer Chemistry Division, National Chemical Laboratory, Pune 411008, India

Received 30 August 2002; accepted 8 January 2003

**ABSTRACT:** Stable, translucent nanolatex with monomer weight % as high as 25 was obtained through emulsion copolymerization of partially water-soluble monomers, ethyl acrylate and methylmethacrylate. The kinetics of reaction, studied at monomer/surfactant (M/S) ratio 10 and 50 showed two intervals and higher rate of particle nucleation for KPS initiated systems. However, AIBN initiated system showed phase separation. The copolymer composition was

determined through <sup>1</sup>H-NMR studies and copolymers showed two glass transition temperatures. Dynamic light scattering studies indicated bimodal distribution of polymer particle size. © 2003 Wiley Periodicals, Inc. *J Appl Polym Sci* 90: 2593–2603, 2003

**Key words:** emulsion polymerization; ethylacrylate; methylmethacrylate; kinetics and particle nucleation

## INTRODUCTION

Emulsion polymerization leads to products with high molecular weights.<sup>1</sup> However, the particle size is reported<sup>2</sup> to be generally greater than 100 nm. Long-term stability of the latexes in some cases is also poor. Reduction in the particle size is desirable, simply because it increases the effective surface area and, therefore, finds numerous applications.<sup>3</sup> Moreover, some specific applications, such as use of nanoparticles as carriers for controlled drug delivery, require the particle size to be smaller than the one generally obtained through emulsion systems.<sup>4</sup> Though microemulsion polymerization is a well-established technique for the production of nanoparticles with very low particle size and narrow particle size distribution, it suffers from the disadvantage of high surfactant concentration.

Our earlier work<sup>5</sup> on polymerization of ethylacrylate (EA) has shown emulsion polymerization as an alternative route for the production of stable nanolatex with particle size comparable to that obtained through microemulsion polymerization. Higher rate of particle nucleation was observed for KPS initiated systems. Pokhriyal et al.<sup>6</sup> also made a similar observation in the emulsion copolymerization of ethylhexyl acrylate–acrylonitrile. Roy and Devi<sup>7</sup> gave a comparative account of the emul-

sion and microemulsion polymerization of MMA/sodium dodecyl sulphate (SDS)/water system. They observed higher isotacticity in the PMMA synthesized through microemulsion polymerization whereas emulsion polymerization resulted in a product with greater syndiotacticity. This was attributed to the difference in the underlying mechanism of polymerization.

Copolymerization in emulsion is a much more complex process as it involves additional parameters like monomer reactivity. In addition, monomer partitioning in case of partially water-soluble monomers makes it more complex. Nevertheless, copolymerization allows a quantitative study of emulsion polymerization with respect to composition and variation in copolymer properties. Capek et al.<sup>8</sup> first investigated the emulsion copolymerization of EA–MMA in the presence of both anionic surfactant spolapan AOS and nonionic emulsifier Tween 40. They reported negligible growth of polymer colloids in the latter stages of emulsion polymerization. It was suggested that copolymerization of partially water-soluble monomers generates new particles by homogeneous nucleation even at higher conversion.

In the present work, we give some experimental evidences for the suggested homogeneous nucleation in the emulsion copolymerization of EA–MMA. The importance of homogeneous nucleation in determining the final particle size and its stability, solid content of latex, and mechanism of copolymerization have also been discussed.

Correspondence to: Surekha Devi (surekha\_devi@yahoo.com).

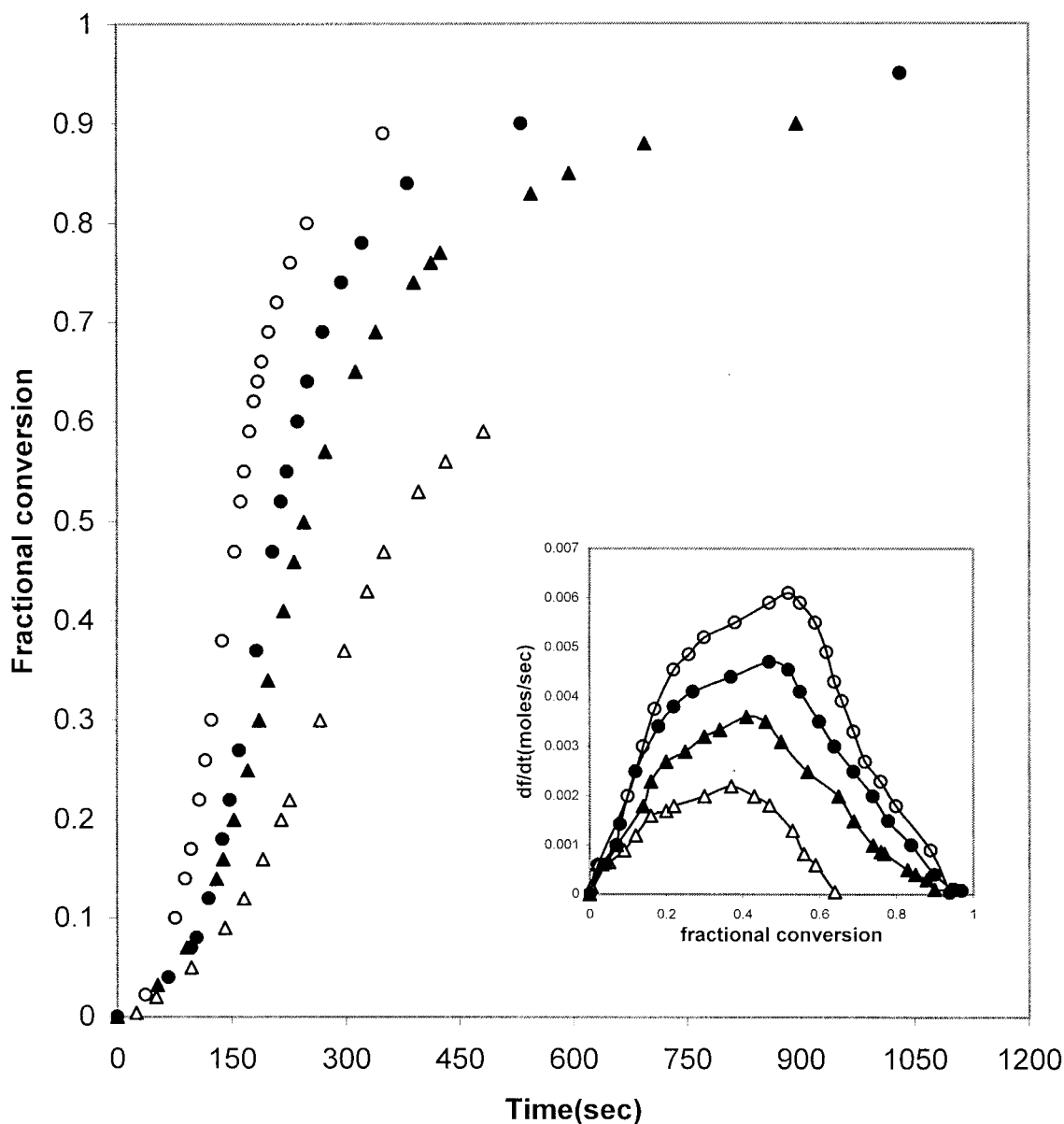


**Figure 1** Effect of KPS concentration on % conversion and rate of polymerization.  $M/S = 10$  and temperature  $70^{\circ}\text{C}$ . ( $\Delta$ ) 0.18 mM, ( $\blacktriangle$ ) 0.36 mM, ( $\bullet$ ) 0.55 mM, ( $\circ$ ) 0.73 mM.

## EXPERIMENTAL

### Materials

EA and MMA from National Chemicals (Baroda, India), was purified by passing through an alumina column and stored at  $4^{\circ}\text{C}$  after vacuum distillation under reduced pressure till further use. SDS extrapure from S.D. Fine Chemicals (Baroda, India) was used as received. Potassium persulphate (KPS) from Sisco Chem (Mumbai, India) was recrystallized from distilled water before use. AIBN from S.D. Fine Chemicals was recrystallized from a mixture of chloroform and methanol.

### Polymerization procedure

#### Kinetics

The batch polymerization in emulsion medium was carried out in a five-neck reaction kettle equipped with a mechanical stirrer, condenser, nitrogen gas inlet, and dropping funnel. The micellar solution containing water and surfactant was stirred for 30 min at the polymerization temperature. This was followed by the addition of monomer over 2 min. The mixture was further stirred for 15 min for emulsification. Requisite quantity of initiator (KPS) was added to the reaction mixture and the kinetics of the reaction was studied by

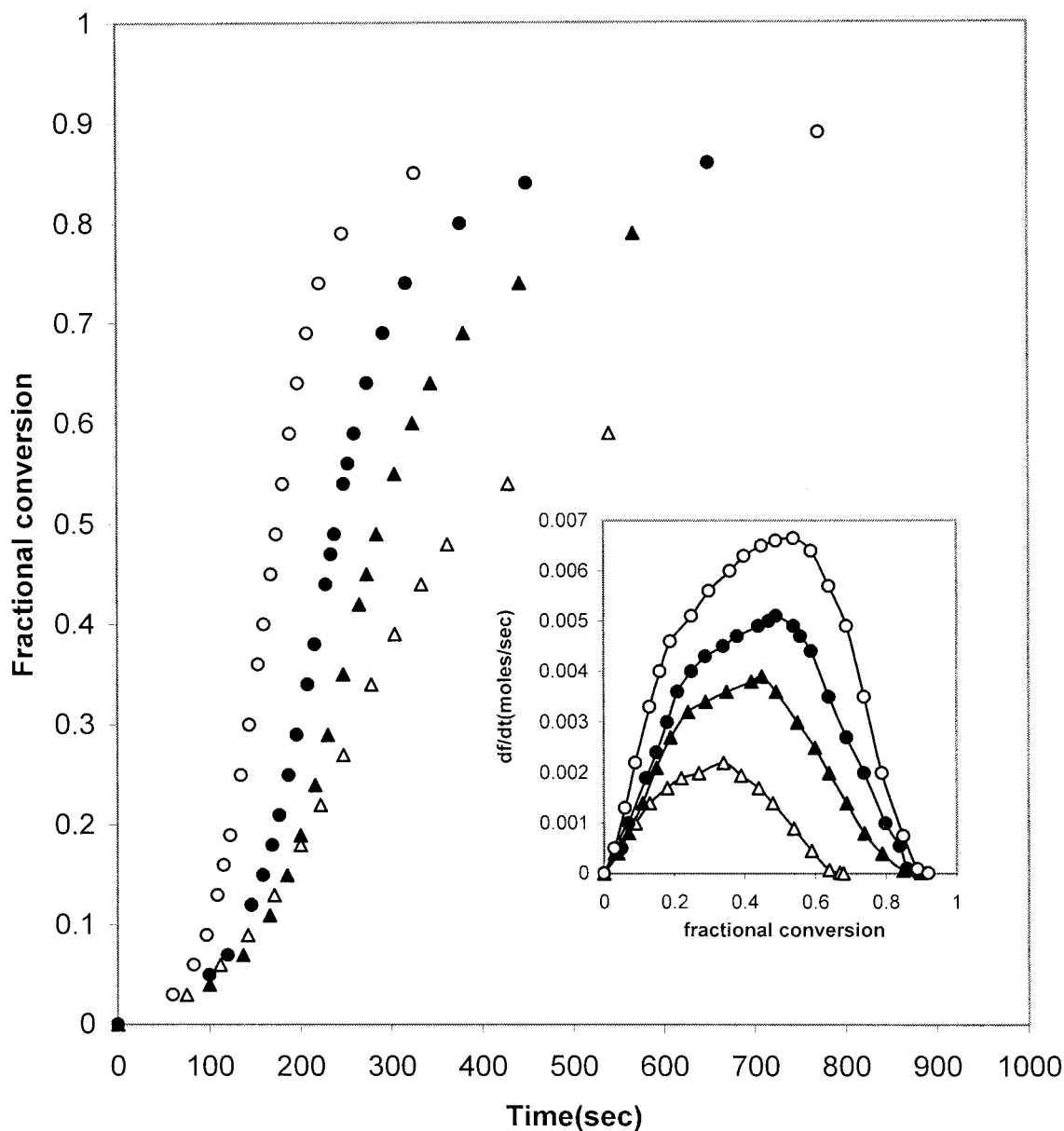


**Figure 2** Effect of KPS concentration on % conversion and rate of polymerization. M/S = 50 and temperature 70°C. ( $\Delta$ ) 0.18 mM, ( $\blacktriangle$ ) 0.36 mM, ( $\bullet$ ) 0.55 mM, ( $\circ$ ) 0.73 mM.

withdrawing the aliquots at regular time intervals. The reaction was quenched by adding 40 ppm of hydroquinone. When AIBN was used as an initiator, it was dissolved in the monomer and added to the reaction mixture. Percentage conversion was determined gravimetrically using methanol as a nonsolvent. The kinetic studies were performed at monomer/surfactant (M/S) ratio 10 and 50. The composition of the respective systems in weight percentages was M/S = 10: 10 EA, 1.0 SDS, 89 water, 0.18–0.73 mM KPS; M/S = 50: 25 EA, 0.50 SDS, 74.5 water, 0.18–0.73 mM KPS.

For the systems initiated with AIBN, concentration used was 0.73 and 12 mM for M/S = 10.

## Characterization

### Spectroscopic analysis

The composition of the copolymer was determined from  $^1\text{H-NMR}$  recorded on 200 MHz Bruker DPX 200 instrument using TMS as an internal reference and 2% w/v solution in  $\text{CDCl}_3$ .

### Thermal analysis

Differential scanning calorimetric (DSC), analysis was carried out on an universal V.2.6D TA instrument at a heating rate of 10°C/min.

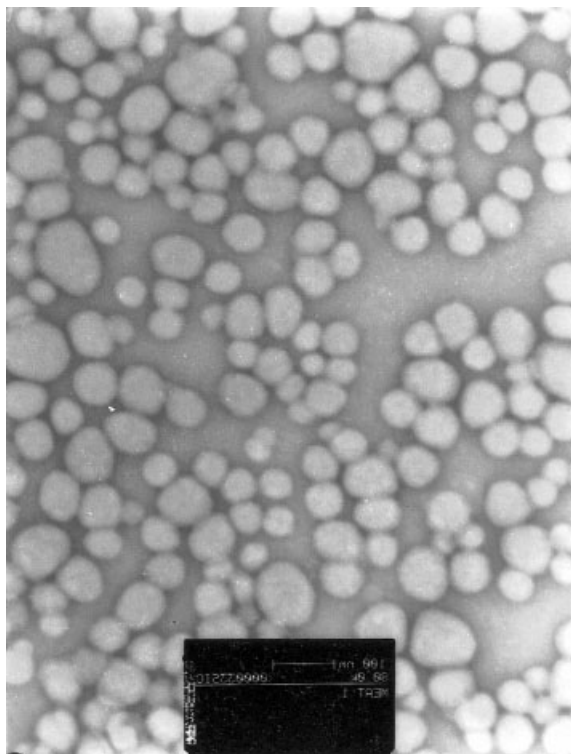


**Figure 3** TEM of EA (0.5)–MMA (0.5) system initiated with 12 mM AIBN for  $M/S = 10$  and temperature  $70^\circ\text{C}$  at 96% conversion and 80 k magnification.

#### Particle size measurements

A Malvern Photon Correlation spectrophotometer, model 4700, equipped with a vertically polarized argon ion laser source operating at 488 nm was used to measure the particle size of the polymerized emulsion latexes in dynamic mode. The scattering intensities from the sample were measured at  $90^\circ$  with the help of a photomultiplier tube. Intensity correlation data were analyzed by the method of cumulants to provide the average decay rate,  $\Gamma = q^2 D$ , where  $q = (4\pi n/\lambda) \sin\theta/2$  is the scattering vector,  $n$  is the index of refraction,  $D$  is the diffusion coefficient, and the variance ( $\nu$ ), which is a measure of the width of the distribution of the decay rate is given as

$$\nu = \frac{\langle \Gamma^2 \rangle - \langle \Gamma \rangle^2}{\langle \Gamma \rangle^2}$$

The measured diffusion coefficients were represented in terms of apparent radii by means of Stokes law. Latexes were diluted up to 100 times and filtered through  $0.2 \mu\text{m}$  Millipore filters before measurements to minimize particle–particle interaction and remove dust particles. The number of particles were, calculated using the following equation:

$$N_p = 6M_0 X_m / \pi \rho D_n^3 \quad (1)$$

where  $D_n$  is a number average diameter of the polymer particles obtained from dynamic light scattering,  $X_m$  is fractional conversion,  $M_0$  is amount of monomer initially charged in  $\text{g}/\text{cm}^3$ ,  $\rho$  is density of polymer in  $\text{g}/\text{cm}^3$ , and  $N_p$  is number of particles/ $\text{cm}^3$ .

Particle sizes of the polymer latexes at 97% conversion were also determined using a Philips Technai-20 transmission electron microscope operated at 200 kV accelerating voltage. The polymerized latexes were diluted 100 times with deionized distilled water and one drop of the diluted dispersion was placed on 200-mesh carbon coated copper grid. Uranyl acetate (2% w/v) was used as a staining agent. Diameters of at least 60 randomly chosen particles were measured directly from the micrograph. The number and weight average diameters were calculated using eqs. (2 and 3), where  $D_i$  is the diameter of the particle and  $n$  is the number of particles measured.

$$D_n = \sum n_i D_i / \sum n_i = \sum n_i D_i / n \quad (2)$$

$$D_w = \sum n_i D_i^4 / \sum n_i D_i^3 \quad (3)$$

#### Molecular weight determination

A Thermo-Quest GPC equipped with Spectra system RI 150 refractive index detector, As-300 auto sampler and Spectra system P100 pump was used along with PSS-GPC software for molecular weight determina-

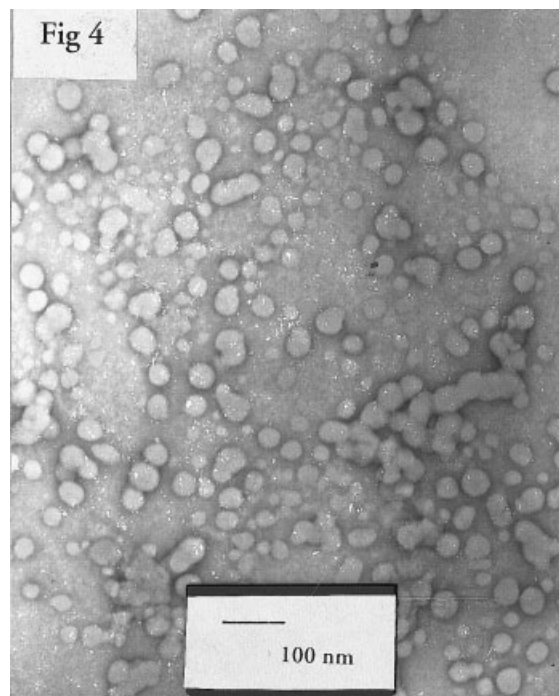


**Figure 4** TEM of EA (0.5)–MMA (0.5) system initiated with 0.73 mM KPS for  $M/S = 50$  and temperature  $70^\circ\text{C}$  at 50% conversion and 80 k magnification.

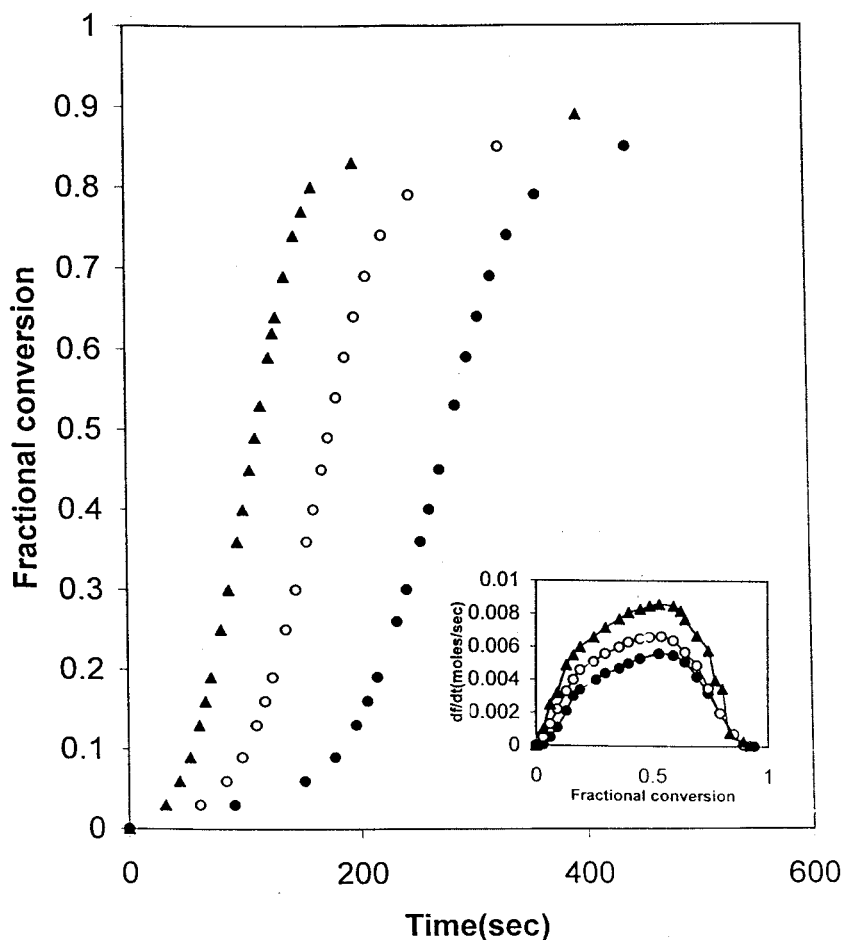


**Figure 5** Effect of monomer feed ratio on the copolymerization kinetics of EA-MMA initiated with 0.73 mM KPS at  $M/S = 50$ . (●) MMA (0.25)-EA (0.75), (○) MMA (0.5)-EA (0.5), (▲) MMA (0.75)-EA (0.25).

tion. HPLC grade THF from S.D. Fine Chemicals was used as a mobile phase at room temperature. Column  $8 \times 600$  mm size, with the stationary phase consisting of two PL Gel SDV  $5 \mu$  linear and  $100 \text{ \AA}$  was used. Twenty microliters of 0.1% polymer solutions were injected to get a neat chromatogram. PMMA with narrow molecular weight distribution (molecular weight range,  $1.4 \times 10^6$ – $3.06 \times 10^2$ ) was used as calibrating standards.

## RESULTS AND DISCUSSION

Emulsion copolymerization of EA-MMA (1:1 mole ratio) was carried out at  $M/S$  ratios 10 and 50. Figures 1 and 2 show the conversion versus time and  $R_p$  versus conversion plots for  $M/S = 10$  and 50, respectively. These emulsions turned into stable, translucent nanosized latexes, when 0.73 mM KPS was used at  $70^\circ\text{C}$ . The latexes were stable against coagulation over a period of 1 year. Such a transition was not observed with AIBN at the same  $M/S$  ratio, initiator concentration, and temperature. Instead, the system showed

phase separation at around 70% conversion. This can be attributed to the lower decomposition rate constant ( $k_d$ ) of AIBN at  $70^\circ\text{C}$  compared to KPS at the same temperature.<sup>9</sup> In addition, due to the partial solubility of AIBN in water, its concentration available for initiation of polymerization in emulsion is significantly less. It is reported that AIBN fraction dissolved in water contributes significantly to the initiation of polymerization and its mechanism is similar to KPS initiation.<sup>10</sup> This leads to the lesser number of active radicals initiating polymerization resulting in the generation of lesser number of polymer particles. Diffusion of monomer from monomer droplets and uninitiated micelles results in the particle growth. The rate of coagulation is also expected to be higher compared to KPS initiated system due to the absence of surface charge on the growing polymer chain generated by AIBN initiation. The combination of these facts makes the available surfactant insufficient, resulting in phase separation. However, use of 12 mM AIBN concentration resulted in stable latex. The latex was analyzed by

**TABLE I**  
Kinetic and Colloidal Parameters for Emulsion  
Copolymerization of EA–MMA Initiated With 0.73 mM  
KPS at M/S Ratio 10 and 50

Fractional conversion	Rate (moles/s)	$D_n$ (nm)	$N_p/cm^3$	$\bar{n}$	$P_I$
M:S = 10					
0.18	0.0038	28	$1.35 \times 10^{15}$	4.66	0.13
0.41	0.0056	33	$1.88 \times 10^{15}$	4.13	0.11
0.76	0.0025	36	$2.7 \times 10^{15}$	1.38	0.10
0.89	0.0009	38	$2.7 \times 10^{15}$	—	0.11
0.95	0.0001	37	$3.06 \times 10^{15}$	—	0.11
M:S = 50					
0.05	0.0011	30	$7.58 \times 10^{14}$	—	0.39
0.17	0.0041	35	$1.62 \times 10^{15}$	2.79	0.08
0.56	0.0065	46	$2.3 \times 10^{15}$	3.73	0.08
0.70	0.0049	50	$2.3 \times 10^{15}$	2.81	0.05
0.86	0.0007	54	$2.3 \times 10^{15}$	—	0.08
0.92	0.0001	57	$2.03 \times 10^{15}$	—	0.11
0.97	0.00002	59	$1.99 \times 10^{15}$	—	0.10

$n$  is average number of radical per particle &  $P_I$  is the polydispersity index.

TEM and number of average diameter of particles was calculated to be 85 nm at 96% conversion (Fig. 3).

It has been reported for water soluble initiators such as KPS that the oligomeric radical formed in aqueous phase can make its entry into the monomer swollen micelle only after the attainment of a critical chain length or hydrophobicity at which it becomes surface active.<sup>11</sup> This can increase its residence time at the micelle water interface and hence the probability of radical entry. For the present system, the critical chain length for entry was calculated from hydrophobic free energy consideration using Maxwell's model.<sup>12</sup>

$$z = 1 - 23 \text{ kJ mol}^{-1}/RT \ln C_w^{\text{sat}} \quad (4)$$

where,  $z$  is the average degree of polymerization for entry,  $C_w^{\text{sat}}$  is the saturated aqueous phase concentration of the monomer in mol/dm<sup>3</sup>. The saturated water solubility reported for EA and MMA is 1.8 and 1.5%, respectively.<sup>1</sup> The average value of  $C_w^{\text{sat}}$  was used for calculation, since 0.5 mole fraction of each monomer was taken for kinetic studies. The calculated value of  $z$  was observed to be 6. Further addition of monomer units to this chain results in the increase in hydrophobic free energy of the surfactant making it hydrophobic enough not to form a micelle but to precipitate out to generate new particle in aqueous phase leading to homogeneous nucleation. It has been reported<sup>13</sup> that the critical degree of polymerization for homogeneous nucleation,  $j_{\text{crit}}$  can be calculated from the consideration of hydrophobic free energy of the surfactant whose Kraft temperature is similar to the temperature of the emulsion polymerization using eq. (5).

$$j_{\text{crit}} = 1 - 55 \text{ kJ mol}^{-1}/RT \ln C_w^{\text{sat}} \quad (5)$$

The value of  $j_{\text{crit}}$  for the present system was observed to be 12 at 70°C. The fact that polymer particles are generated by both micellar and homogeneous nucleation is evident from the following studies.

### Reaction kinetics

The  $R_p$  versus conversion plots (Figs. 1 and 2) show a prolonged nucleation period and the absence of a generally observed constant rate period in classical emulsion polymerization. The emulsion system turned translucent in the range of 35–40% conversion. TEM (Fig. 4) for a 50% conversion sample (soon after the system turned translucent) shows a large number of smaller particles most likely to be generated by homogeneous nucleation for M/S = 50 system. Since the conversion of micelles into polymer particles takes place at lower conversion, the further increase in the rate of polymerization can be attributed to particle nucleation in aqueous phase (homogeneous nucleation). The slower increase in rate due to particles generated through homogeneous nucleation has been attributed<sup>14</sup> to reduced swelling of the particles by monomer due to their hydrophilic character and rapid exit of free radicals due to their small size. Simultaneous diffusion of monomer into the particles generated via micellar and homogeneous nucleation results in the disappearance of monomer as a separate phase by the time the rate maxima is achieved. Due to higher rate of particle nucleation, particle growth kinetics becomes less important in these emulsion systems involving both partially water soluble monomers. Two-stage kinetics in emulsion polymerization has been reported even in the case of styrene and SDS as a surfactant by Varela de la Rosa et al.<sup>15</sup> where the conversion was monitored by a microcalorimeter. Gan et al. also have reported two-stage kinetics in the emulsion polymerization of styrene and MMA.<sup>16</sup>

**TABLE II**  
Molecular Weight Through GPC and Particle Size Data  
From DLS and TEM for EA (0.5)–MMA (0.5) Copolymers  
at M/S = 10 and 50

	M/S:10	M/S:50
By GPC		
$M_w$	$5.19 \times 10^5$	$1.34 \times 10^6$
$M_n$	$1.63 \times 10^5$	$5.09 \times 10^5$
$M_w/M_n$	3.17	2.64
By TEM		
$D_w$ (nm)	40	63.15
$D_n$ (nm)	39	61.32
$D_w/D_n$	1.01	1.02
By DLS		
$D_2$ (nm)	42.4	64.2

**TABLE III**  
**Composition Derived From <sup>1</sup>H-NMR Studies of EA/MMA Copolymers Synthesised in Bulk and Emulsion**

Feed concentration		Emulsion (M/S = 50)		Emulsion (M/S = 10)		Bulk	
$f_{EA}$	$f_{MMA}$	$F_{EA}$	$F_{MMA}$	$F_{EA}$	$F_{MMA}$	$F_{EA}$	$F_{MMA}$
0.90	0.10	0.81	0.19	0.76	0.24	0.72	0.27
0.75	0.25	0.58	0.42	0.54	0.46	0.51	0.49
0.66	0.33	0.48	0.52	0.43	0.57	0.42	0.57
0.50	0.50	0.35	0.65	0.32	0.68	0.30	0.70
0.25	0.75	0.19	0.81	0.14	0.86	0.13	0.86
0.10	0.90	0.10	0.90	0.06	0.94	0.05	0.94

$f_{EA}, f_{MMA}$ : Feed concentrations of ethylacrylate (EA) and methylmethacrylate (MMA).  $F_{EA}, F_{MMA}$ : EA and MMA fraction in copolymer synthesized through emulsion and bulk polymerization.

However, to the best of our knowledge, no explanation is offered for the observation.

Increase in the initiator concentration increases the free radical flux. As a result the fraction of micelles that capture the free radicals to become active particles increases, leading to increased rate of polymerization.

The dependency of  $R_p$  on initiator concentration was found to be 0.72 and 0.81 for M/S = 10 and 50, respectively. The observed deviation from the 0.4 exponent proposed by Smith and Ewart<sup>17</sup> for hydrophobic monomer styrene, can be explained on the basis of requirement of growth of primary free radicals in

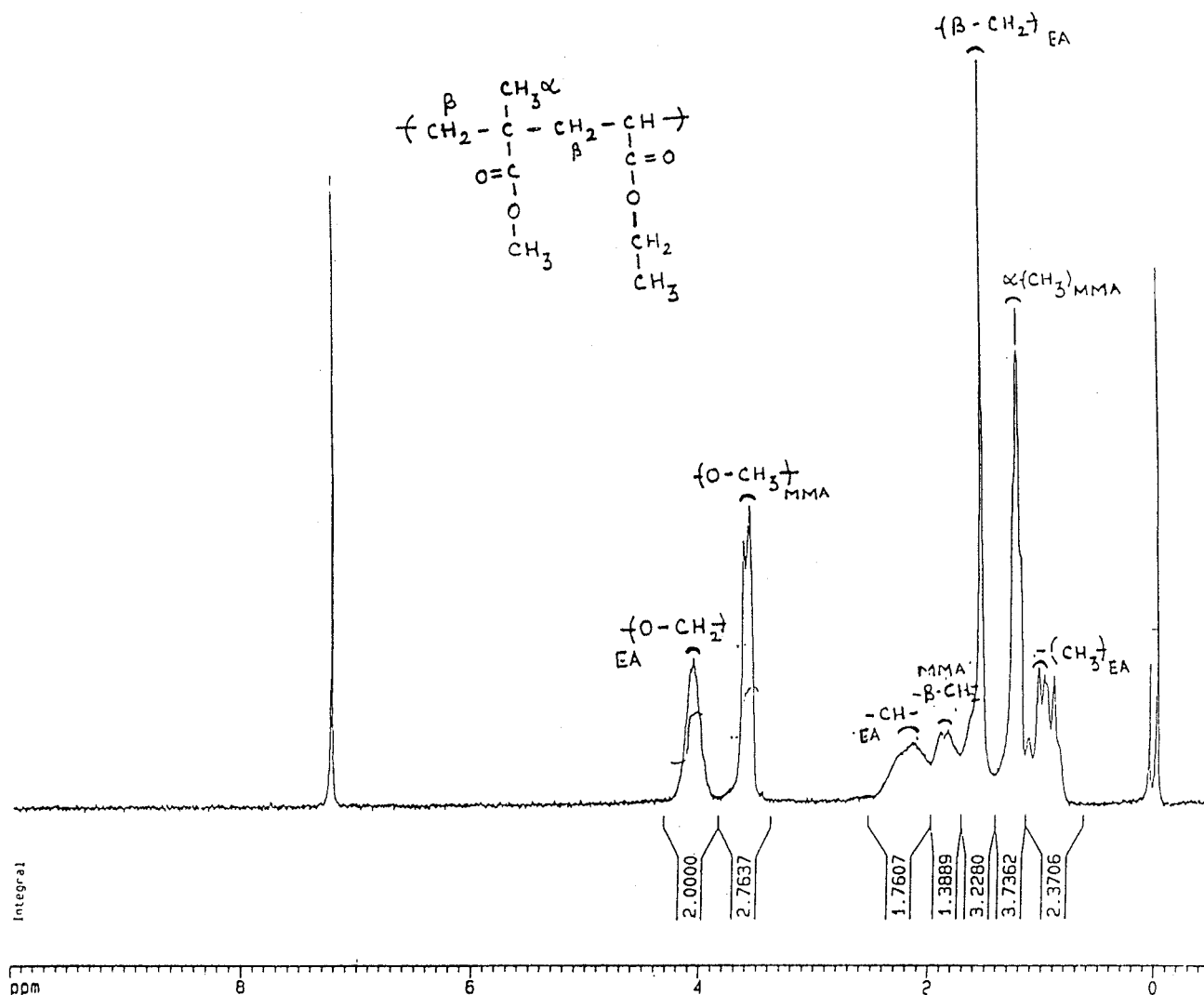


**Figure 6** <sup>1</sup>H-NMR spectra of EA-MMA copolymers synthesized through emulsion polymerization. MMA in feed 0.5 and in copolymer 0.651.

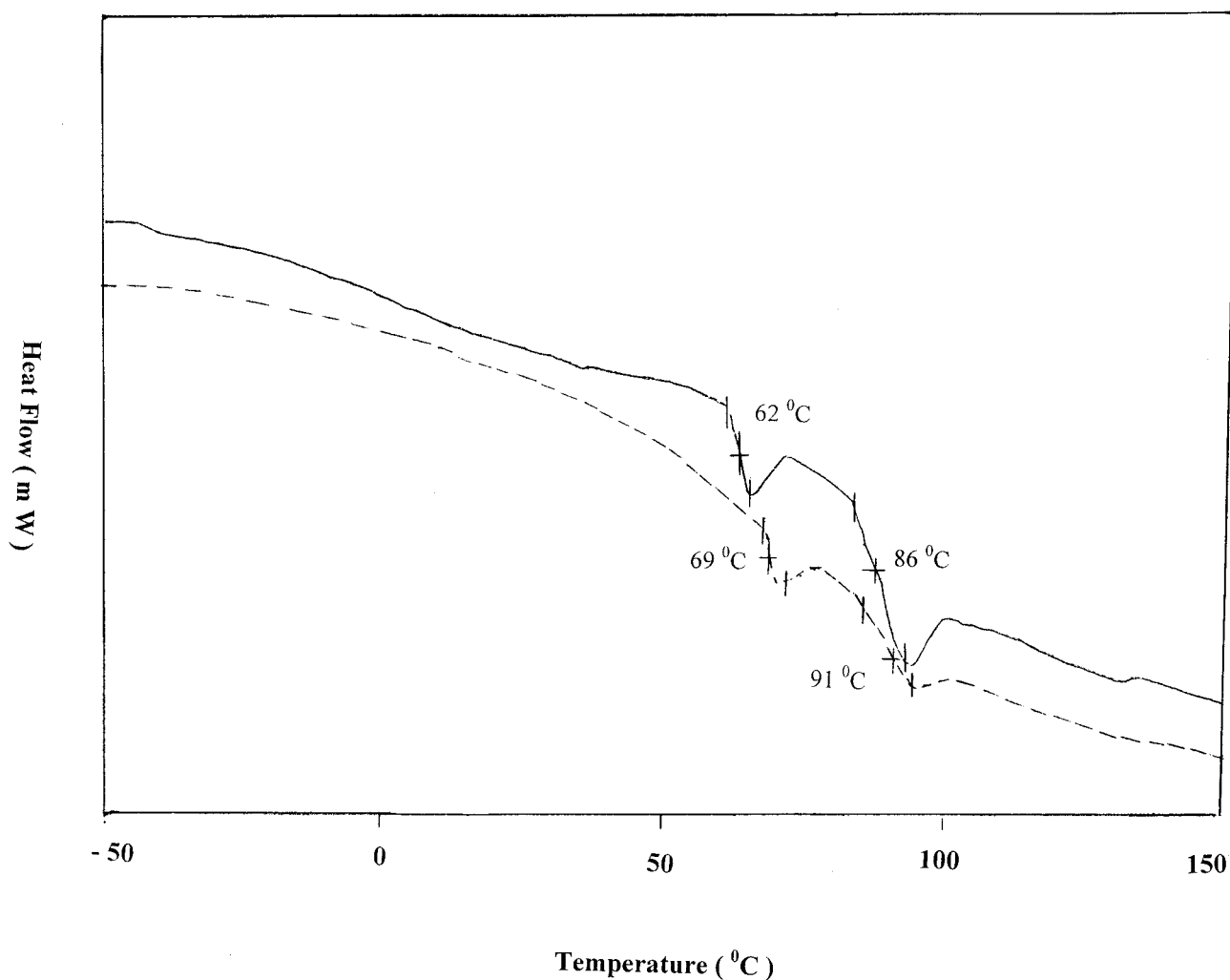


Figure 7 DSC thermograms of EA (0.5)/MMA (0.5) copolymer synthesized through emulsion polymerization. M/S ratio 10 (.....) and M/S ratio 50 (—) at conversion below 10%.

aqueous phase to a certain chain length before entering into micelles. Once the critical chain length is attained, the oligomer can contribute to particle nucleation through the entry into micelle, or it may form micelles by aggregating with the free or desorbed surfactant molecules or else it will grow and precipitate as primary particles in aqueous phase (homogeneous nucleation).<sup>13</sup> All these possible processes will make the rate of polymerization more sensitive to initiator concentration when polar monomers are used. Copolymerization kinetics studied at three different feed ratios (Fig. 5) also shows similar nature of the rate plot. Increase in MMA in the feed increases the rate of polymerization due to higher reactivity of MMA in the presence of EA. Particle stability in these systems is provided by the products of aqueous phase termination events and the available surfactant. For a given surface area, polar polymers require lesser amount of emulsifier in comparison to a hydrophobic polymer like styrene. Therefore, a greater number of

particles can be stabilized with the same amount of surfactant.

#### Probable termination

The number of radicals per particle ( $n$ ) for the system under study was calculated using the following equation, and the results are given in Table I.

TABLE IV  
Effect of Copolymer Composition on  $T_g$ 's for M/S = 10 and M/S = 50 System

Composition		M/S = 10		M/S = 50	
EA	MMA	$T_g$ (°C)	$T_g$ (°C)	$T_g$ (°C)	$T_{g2}$ (°C)
0.25	0.75	72	100	68	102
0.50	0.50	69	91	62	86
0.75	0.25	28	66	23	71
0.90	0.10	0.30	50	-1.0	68



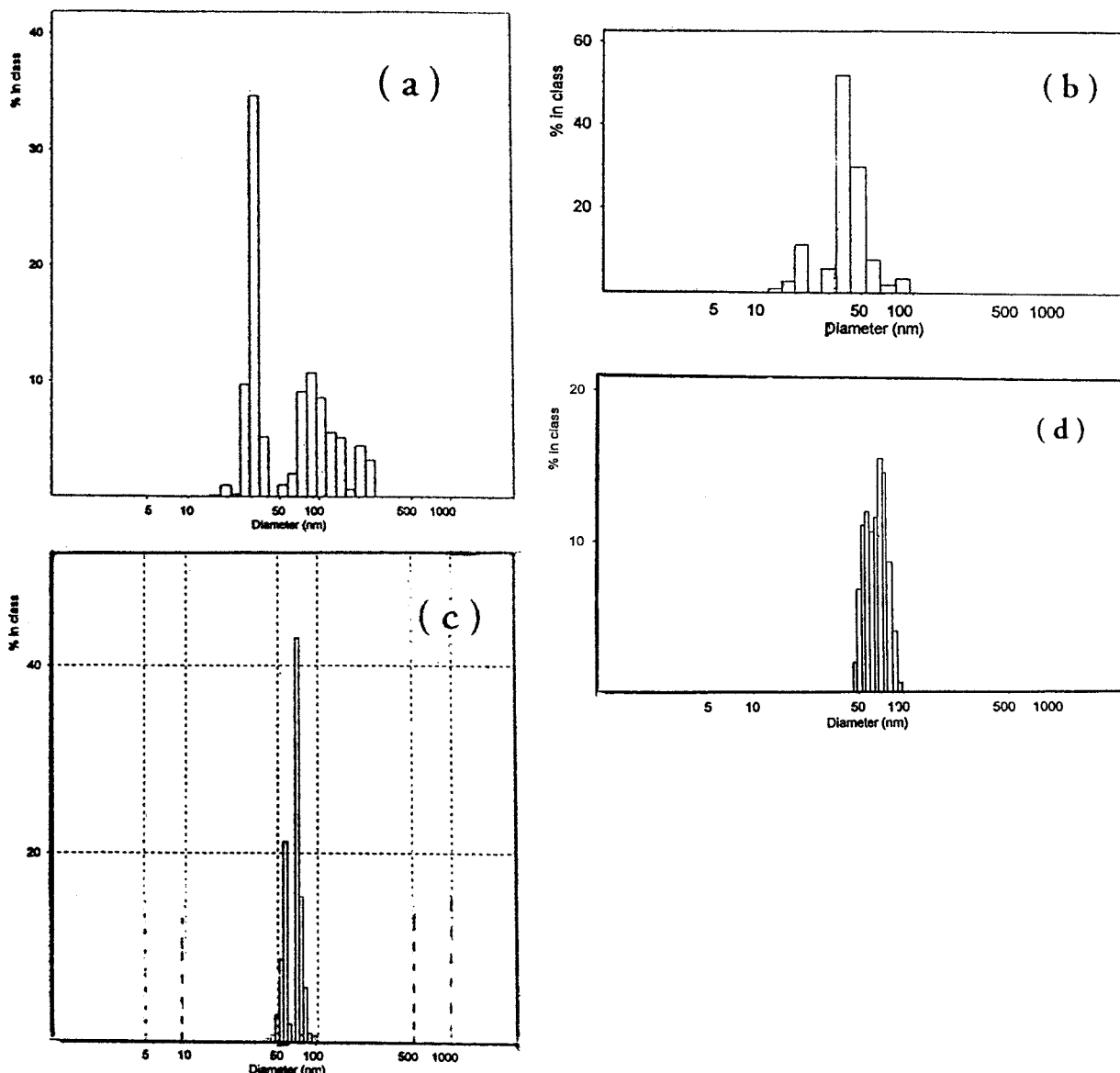


Figure 8 Particle size distribution of EA (0.5)-MMA (0.5) copolymer synthesized through emulsion polymerization at M/S = 50 at various conversions initiated with 0.73 mM KPS. (a) 4%, (b) 27%, (c) 57%, (d) 97%.

$$\bar{n} = \frac{R_p(c) \times N \times (k_{PEA} \times r_{MMA} + k_{PMMA} \times r_{EA} \times L) \times (1 + L)}{[M]_{eq} \times k_{PMMA} \times k_{PEA} \times N_p \times (r_{MMA} + 2L + r_{EA} \times L^2)} \quad (6)$$

where  $[M]_{eq}$  is the equilibrium monomer concentration, taken as 6.0 mol/dm<sup>3</sup> as reported by Capek et al.<sup>8</sup> from the swelling studies of the final MMA-EA copolymer latices. The reported<sup>8</sup> propagation rate constant ( $k_p$ ) values of 1,500 and 686 dm<sup>3</sup> mol<sup>-1</sup> s<sup>-1</sup>, for EA and MMA have been used for the calculation of  $n$ . The monomer ratio [EA]/[MMA], is represented as  $L$ . Reactivities of EA and MMA used for calculation in emulsion medium are reported to be 0.25 and 1.44 respectively by us ear-

lier.<sup>18</sup>  $N_p$  is the number of particles calculated from eq. (1) using dynamic light scattering data Table II.

The final particle size obtained by TEM was 39 and 61 nm for M/S = 10 and 50. However, the number of polymer chains per particle ( $n_p$ ) was observed to be 35 and 135 for M/S = 10 and 50, respectively. The higher value of  $n_p$  can arise due to the larger volume of the particles and lower molecular weight resulting from a higher frequency of radical entry, as a fewer number of polymer particles are available.

### <sup>1</sup>h-nmr study

Even the small difference in solubility of EA (1.8%) and MMA (1.5%) has shown considerable influence in

the copolymer composition as seen from NMR studies and thermal properties. The copolymer composition data for emulsion polymerization obtained by  $^1\text{H-NMR}$  at various feed compositions and below 10% conversion is given in Table III. The copolymers synthesized through emulsion polymerization showed greater fraction of the more water-soluble monomer EA in comparison to the copolymer synthesized by bulk polymerization of EA-MMA<sup>19</sup> for identical feed concentration and below 10% conversion. This indicates composition drift in emulsion polymerization, which arises due to the initiation of polymerization in both aqueous phase and micelles. The copolymer composition studied at  $M/S = 10$  for conversion below 10% and at various compositions shows lesser drift in copolymer composition compared to  $M/S = 50$  (Table III). A representative NMR for EA-MMA copolymer is given in Figure 6.

#### Dsc study

The copolymers synthesized through emulsion polymerization show two  $T_g$ 's (Fig. 7 and Table IV). Appearance of two  $T_g$ 's can be attributed to the formation of a diblock copolymer due to large difference in the monomer reactivities<sup>18</sup> ( $r_{\text{MMA}} = 1.44$ ,  $r_{\text{EA}} = 0.25$ ). However, such a possibility can be denied as the polymer characterization is done below 10% conversion and copolymer synthesized in microemulsion showed single  $T_g$ .<sup>18</sup> Hence the appearance of two  $T_g$ s confirms the formation of two types of copolymer chains with different composition arising from micellar and homogeneous nucleation. The polymer generated via micellar polymerization is expected to have a greater fraction of the less water soluble monomer, MMA and corresponds to the higher  $T_g$ . Whereas, homogeneous nucleation generates polymer chains with higher fraction of the more water soluble monomer, EA resulting in the lower  $T_g$ . The difference in observed  $T_g$ s is significant due to the large difference in the  $T_g$ s of the homopolymers.

#### Dynamic light scattering

The observed bimodal distribution of particles particularly at lower conversions (Fig. 8) also indicates particle generation through two nucleation mechanisms. Particles generated by homogeneous nucleation are relatively unstable in a colloidal state, which is reported<sup>14</sup> to arise as a consequence of their small size and extreme curvature of electrical double layer. Therefore, the particles are likely to coagulate leading to a slight increase in particle size and monodispersity as seen in TEM (Fig. 9) and particle size distribution for a 97% conversion sample [Fig. 8(d)]. Table I shows the final number of particles ( $N_p$ /mL) for the system

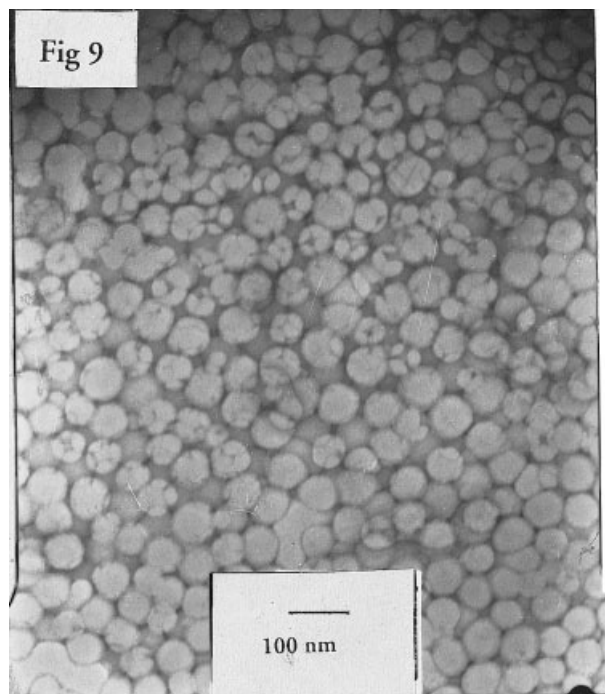


**Figure 9** TEM of EA (0.5)-MMA (0.5) system initiated with 0.73 mM KPS for  $M/S = 50$  and temperature 70°C at 97% conversion and 80 k magnification.

with  $M/S$  ratio 10 and 50. Number of particles was observed to increase initially and thereafter remained nearly constant.

#### CONCLUSIONS

Emulsion system with  $M/S$  ratio 10 and 50 could be turned into stable translucent nanolatexes, with monomer content as high as 25 wt % for KPS initiated systems. The rate of particle nucleation was observed to be higher than the rate of particle growth resulting in larger number of smaller particles stabilized by the available surfactant. Appearance of two  $T_g$ s and NMR data suggests that particle generation in emulsion polymerization takes place both via homogenous and micellar nucleation. Higher rate of particle nucleation allows the formation of stable nanolatexes in the size range otherwise obtained through microemulsion polymerization but with much lower surfactant and higher monomer concentration.

Interestingly, same molar concentration of AIBN shows separation of two phases due to lower rate of particle nucleation and higher rate of particle growth.

Authors gratefully acknowledge the financial support for this work from University Grants Commission, New Delhi, India. Authors also thank Dr. S. Sivaram, Director, NCL, Pune for providing light scattering facility.

**References**

1. Lovell, P. A.; El-Aasser, M. S. *Emulsion Polymerization & Emulsion Polymers*; John Wiley: New York, 1997; Vol. 45, p 211.
2. Arzamendi, G.; Leiza, J. R.; Asua, J. M. *Macromol Chem* 1986, 187, 2063.
3. Hiemenz, P. C.; Rajagopalan, R. *Principles of Colloid and Surface Chemistry*, 3rd ed. Marcel Dekker, Inc., New York, 1997; Chapter 1.
4. Larpent, C.; Richard, J.; Vaslin-Reimann, S. *PCT Int Appl WO* 1993, 93 24, 534 (to Prolabo).
5. Bhawal, S.; Pokhriyal, N. K.; Devi, S. *Eur Polym J* 2002, 38, 735.
6. Pokhriyal, N. K.; Sanghvi, P. G.; Shah, D. O.; Devi, S. *Langmuir* 2000, 16, 5864.
7. Roy, S.; Devi, S. *J Appl Polym Sci* 1996, 62, 1509.
8. Capek, I.; Tuan, L. Q. *Macromol Chem* 1986, 187, 2063.
9. Brandrup, J., Immergut, E. H. *Polymer Handbook*, 3rd ed.; Wiley: New York, 1989.
10. Nomura, M.; Fujita, K. *Makromol Chem Rapid Commun* 1989, 10, 581.
11. Morrison, B. R.; Maxwell I. A.; Napper, D. H.; Gilbert, R. G.; Ammerdorffer, J. L.; German A. L., *J Polym Sci Polym Chem Ed* 1993, 31, 467.
12. Maxwell, I. A.; Morrison, B. R.; Napper, D. H.; Gilbert, R. G. *Macromolecules* 1991, 24, 1629.
13. Gilbert, R. G. *Emulsion Polymerization: A Mechanistic Approach*; Academic Press: London, 1995, 309, 15.
14. Feeney, P. J.; Napper, D. H.; Gilbert, R. G. *Macromolecules* 1984, 17, 2520.
15. Varela de La Rosa, L.; Sudol, E. D.; El-Aasser, M. S.; Klein, A., *J Polym Sci Part A Polym Chem* 1996, 34, 461.
16. Gan, L. M.; Chew, C. H.; Ng, S. C.; Loh, S. E. *Langmuir* 1993, 9, 2799.
17. Smith, W. V.; Ewart, R. H. *J Chem Phys* 1948, 16, 592.
18. Bhawal, S.; Devi, S. *J Appl Polym Sci* (to appear).
19. Gressie, N.; Torrance, B. J. D.; Fortune, J. D. *Polymer* 1965, 6, 653.